07.4

Spintronic emitter of terahertz radiation based on two-dimensional semiconductor tungsten diselenide

© A.M. Buryakov[1], A.V. Gorbatova[1], P.Yu. Avdeev[1], N.V. Bezvikonny[1], S.V. Ovcharenko[1], A.A. Klimov[1], K.L. Stankevich[2], E.D. Mishina[1]

[1] MIREA — Russian Technological University, Moscow, Russia
[2] Kotelnikov Institute of Radio Engineering and Electronics, Russian Academy of Sciences, Moscow, Russia
E-mail: buryakov@mirea.ru

Received May 11, 2022
Revised July 26, 2022
Accepted July 28, 2022

We propose a new spintronic emitter based on the Co/WSe_2 heterostructure. The time of ultrafast demagnetization is estimated. It is shown that the two-dimensional ferromagnet/semiconductor interface exhibits strong spin-orbit coupling. Approaches to the description of the mechanism of generation of THz radiation are implemented. It is shown that the polarization orientation of THz radiation depends on the direction of magnetization

Keywords: Spintronic emitter, THz radiation, two-dimensional semiconductors, Co/WSe_2, THz polarization.

DOI: 10.21883/TPL.2022.09.55084.19246

Advancements in terahertz (THz) technology translated into such promising applications as nondestructive testing [1], chemical analysis [2], wireless THz communication [3,4], and medical diagnostics [5]. The latest research at the confluence of THz generation and spintronics resulted in the discovery of a new class of THz sources controllable by both spin and charge currents [6,7]. Metallic spintronic THz emitters based on ferromagnetic (FM)/non-magnetic (NM) heterostructures currently demonstrate the greatest potential among all THz sources [7]. Spin current $\mathbf{j}_s$ produced in an FM material under the influence of a femtosecond laser pulse flows within an NM layer and is converted there into transverse charge current $\mathbf{j}_c = \alpha_H \mathbf{j}_s \times \mathbf{M}/|\mathbf{M}|$ ($\mathbf{M}$ is the FM magnetization and α_H is the spin Hall angle characterizing the deflection of an electron [8]) due to the inverse spin Hall effect (ISHE). The generated THz wave field is $\mathbf{E}_{\mathrm{THz}}(t) \sim \partial \mathbf{j}_c(t)/\partial t$. FM/semiconductor (SC) systems attract special interest [9–11]. The SC properties allow one to achieve a strong spin polarization of current: only the electrons with the majority spin and an energy above the SC conduction band minimum cross the FM/SC interface, while minority electrons are subjected to rapid thermalization.

In the present study, a spintronic THz emitter based on a Co/WSe_2 heterostructure is proposed. A two-dimensional tungsten diselenide semiconductor was chosen for the fact that W provides a stronger internal spin-orbit interaction than Mo [12]. This ensures that the spin current in a semiconductor gets converted due to spin-orbit effects into the charge current (Rashba effect), which contributes to THz generation alongside with ISHE.

A multilayer tungsten diselenide (WSe_2) film was grown by chemical vapor deposition on a silicon substrate (Six Carbon Technology Co., Ltd.). The sample was 10×10 mm in size. The fraction of the sample surface covered by a monolayer was 95%. A thin cobalt layer with a thickness of 5 nm was deposited onto the WSe_2/Si surface by magnetron sputtering and covered by a protective SiO_2 layer with a thickness of 3 nm. The schematic diagram of the sample in the laboratory frame of reference is shown in Fig. 1, *a*. The fabricated SiO_2 (3 nm)/Co (5 nm)/WSe_2/Si heterostructure was characterized by atomic force microscopy (AFM). Its thickness was verified via ellipsometry (a LEF-777 ellipsometer was used). The mean-square surface roughness (Fig. 1, *b*) was $R_{rms} \sim 0.8$ nm. Magnetic characteristics were measured using the ferromagnetic resonance (FMR) technique with a Bruker spectrometer at frequency $\omega/2\pi = 9.74$ GHz and $T = 300$ K. FMR line $H_{res} = 811$ Oe with FWHM $\Delta H = 325$ Oe was detected this way. The Co film magnetization was calculated based on the obtained data in accordance with the classical Kittel formula for a magnetizing field: $4\pi M = 13\,190$ G.

THz emission parameters were examined using the standard THz time-domain spectroscopy technique in the „reflection“ configuration. This emission was excited by linearly polarized femtosecond laser pulses with a wavelength of 800 nm, a duration of 35 fs, and a repetition rate of 3 kHz („Katyusha“ titanium-sapphire laser, Avesta, Russia). The excitation beam was incident on the surface at an angle of 45° to the normal. The maximum energy density was $1.7\ \mathrm{mJ} \cdot \mathrm{cm}^{-2}$. The experimental setup and the mechanism of detection of THz radiation with an electrooptical ZnTe crystal were discussed in detail in [13–15].

Hysteresis curves of the THz signal amplitude and magnetic hysteresis curves are shown in Fig. 2, *a*. The field dependence of the THz signal was measured at point $t = 0$ ps. The temporal dynamics of generated THz pulses typical of Co/WSe_2 is presented in the inset of Fig. 2, *b*.

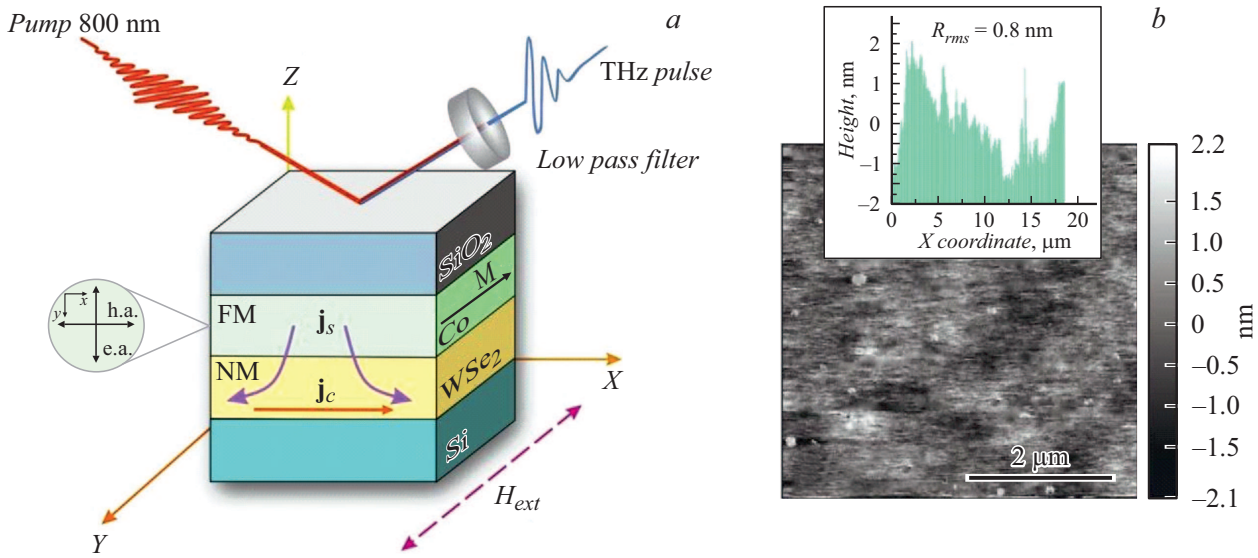

Figure 1. *a* — Schematic diagram of the sample in the laboratory frame of reference (FM — ferromagnetic material, NM — non-magnetic material); *b* — AFM image of the sample surface.

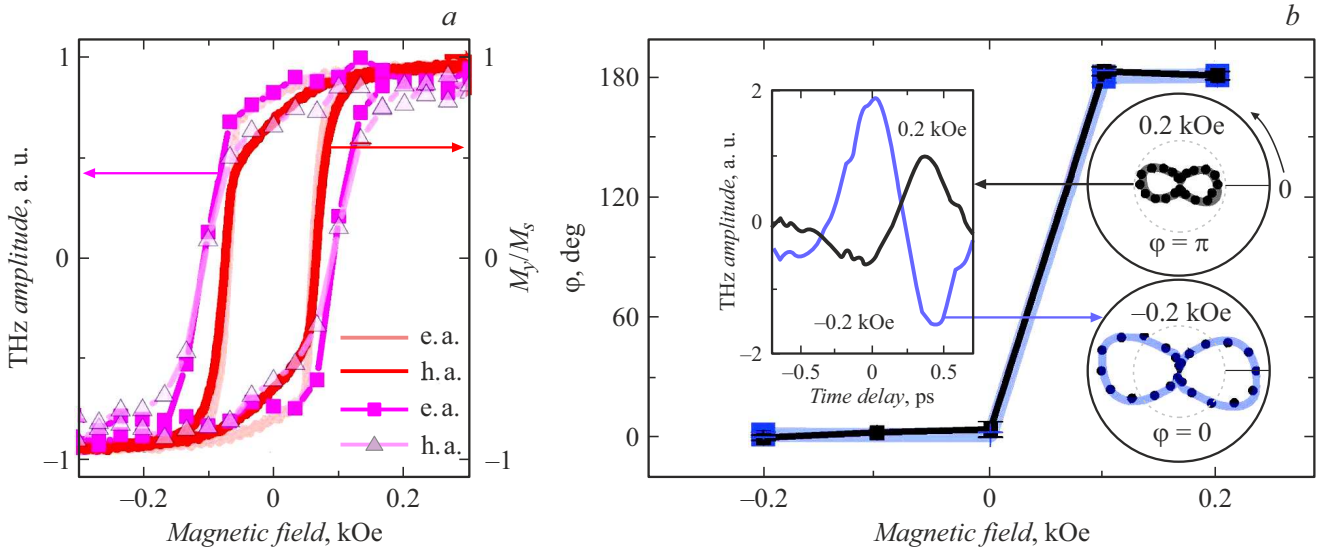

Figure 2. *a* — Hysteresis curves of the THz signal amplitude obtained at the maximum point for a time delay of 0 ps (lines with symbols) and hysteresis curves of magnetization $M_y(H)$ (lines without symbols). *b* — Rotation of polarization of THz radiation as a function of the applied magnetic field in the HA geometry.

The magnetic field was applied parallel to axis Y of the laboratory frame of reference (Fig. 1, *a*) and normally to the optical beam incidence plane (XZ). Hysteresis curves were measured for two variants of geometric positioning of the sample relative to the external magnetic field: along the „easy“ axis (EA) and along the „hard“ axis (HA). We have demonstrated in our earlier study [15] that magnetization curves match perfectly the parameters of the THz signal amplitude hysteresis for TbCo/FeCo structures. Similar results were obtained by the authors of [16] for the $Co_{40}Fe_{40}B_{20}$ (1.8 nm)/Pt (2 nm) structure. The matching of parameters of hysteresis curves of the THz signal amplitude and magnetization curves is typical only of metallic spintronic THz emitters where the emission is governed by ISHE. The magnetization curve for the Co/WSe_2 structure, which is shown in Fig. 2, *a* (lines without symbols), and the corresponding THz signal amplitude hysteresis (lines with symbols) differ by 30% in terms of the coercive field. This field is approximately 0.1 kOe for the THz signal amplitude hysteresis and roughly equal to 0.07 kOe for the magnetization curve. The observed magnetic hysteresis of the THz signal amplitude is related to a change in the magnetization direction. This verifies the spin nature of THz generation in the studied structure. A change in the polarity

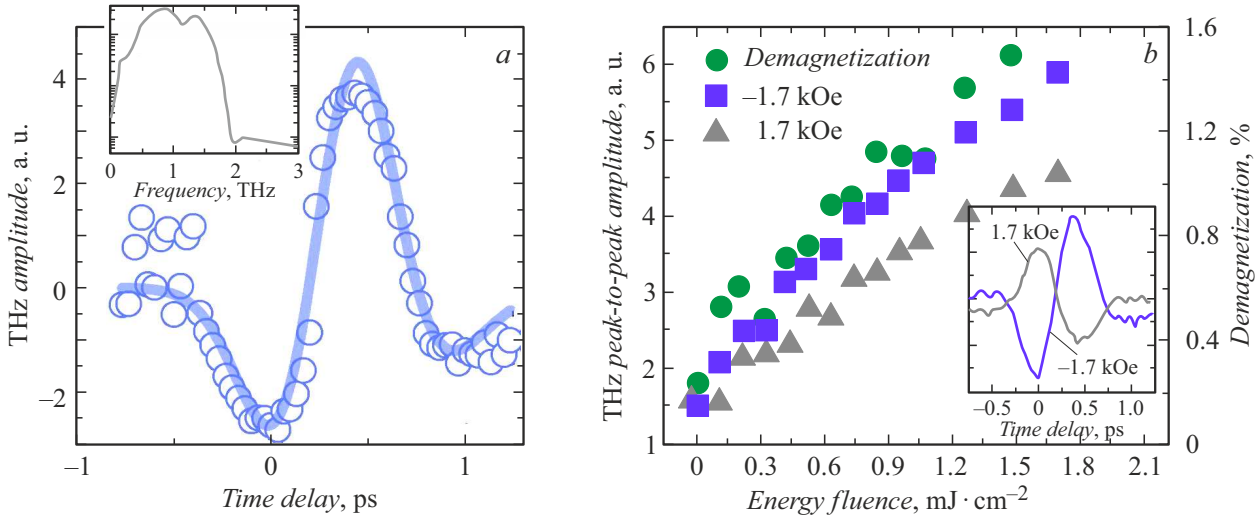

Figure 3. *a* — Temporal dynamics of the THz signal. The frequency spectrum of this signal obtained via the Fourier transform is shown in the inset. *b* — Dependences of the peak-to-peak THz amplitude and ultrafast demagnetization on the energy density of the excitation laser pulse for a magnetic field of ± 1.7 kOe. The THz signal dynamics determined at an energy density of $\sim 1.7\,\mathrm{mJ \cdot cm^{-2}}$ for different polarities of the applied magnetic field is shown in the inset.

of the external magnetic field in transition from the region of negative saturation $-H_s$ to the region of positive saturation $+H_s$ is accompanied by a 180° rotation of THZ polarization, which is typical of spintronic emitters (inset of Fig. 2, *b*). Figure 2, *b* shows the dependence of the rotation angle of the THz polarization plane on the applied external magnetic field. The THz polarization rotation angle was determined by approximating polarization dependences of the peak-to-peak THz signal amplitude (the sum of maximum and minimum values of the THz signal amplitude) in accordance with the approach detailed in [17]. Polarization dependences of the peak-to-peak THz signal amplitude were obtained by rotating a grating polarizer that intercepts the THZ beam between the generator and the ZnTe detector crystal. Typical polarization dependences of the THZ signal measured in negative and positive saturation regions are presented in Fig. 2, *b*. The initial position in the angular dependences in Fig. 2, *b* corresponds to a THz beam polarization lying in incidence plane *XZ*. It can be seen that the transition to the region of positive saturation is accompanied by a 180° rotation of THZ polarization. The coercive field in this case does not exceed 0.1 kOe. In addition, it was demonstrated in [18] that the amplitude of a THz signal generated by thin cobalt films reaches its peak at a thickness of ~ 40 nm. When the cobalt film thickness was reduced further to 5 nm, the signal amplitude dropped by 90% of the initial value. The presence of magnetic hysteresis and THz radiation provides evidence of the effects occurring at the Co/WSe_2 interface: injection of spins from the ferromagnetic layer to the semiconductor, inverse spin Hall effect, and Rashba effect.

The generation of THz radiation by the spintronic emitter in a magnetic field of 1.7 kOe is illustrated by Fig. 3, *a*. The peak-to-peak THz signal amplitude for Co/WSe_2 is higher than the one that was measured in our earlier study [14] for FeCo/TbCo structures. It was demonstrated in [14] that the inverse spin Hall effect, which is induced by a non-magnetic conducting metal, is the primary mechanism of THz generation in the magnetic superlattice/non-magnetic metal structure. It should be noted that this structure design is traditional for spintronic emitters and provides the highest efficiency of THz generation. In the present study, the magnetic/semiconductor structure yields better results at markedly lower values of conductivity of the demagnetizing layer (semiconductor/non-magnetic metal). The frequency spectra of generated THz signals are shown in the inset of Fig. 3, *a*. The frequency spectrum width is limited by the spectral sensitivity range of ZnTe and is equal to 3 THz. Figure 3, *b* presents the dependences of the peak-to-peak THz wave amplitude on the laser pumping energy density for a magnetic field of ± 1.7 kOe. Since THz radiation is associated with ultrafast demagnetization, dependences of the magnitude of this demagnetization and the THz radiation amplitude on the excitation radiation energy density are expected to be related. If one assumes that pumping pulses excite elementary magnetic dipoles in a film coherently and produce a time-variable magnetization, the radiated electric far-field polarized in direction x is defined as [19]

$$E_x(t) = \frac{\mu_0}{4\pi^2 r}\frac{\partial^2 M_x}{\partial t^2}\left(t - r/c\right), \qquad (1)$$

where r is the distance to the radiation source. The following phenomenological expression was used for the time dependence of ultrafast demagnetization [19]:

$$\Delta M(t) = \{-\theta(t)[k_1(1 - e^{-\frac{t}{\tau_1}})e^{-\frac{t}{\tau_2}} + k_2(1 - e^{-\frac{t}{\tau_2}})]\} \otimes G(t), \qquad (2)$$

where t is time, $\Delta M(t)$ is time-dependent demagnetization, $\theta(t)$ is the Heaviside function, k_1 and k_2 are constants specifying the ultrafast demagnetization magnitude, τ_1 and τ_2 are the demagnetization time and the time of magnetization relaxation to the initial state, and $G(t)$ is the Gauss function.

An example of the approximated time dependence of the THz radiation amplitude for an excitation radiation energy density of $1.7\,\mathrm{mJ}\cdot\mathrm{cm}^{-2}$ is shown in Fig. 3, *a*. The enhancement of generation efficiency of the presented spintronic emitter relative to the efficiency of a spintronic emitter produced by exfoliation of transition metal dichalcogenide (TMD) layers on a cobalt surface [20] was 14%. THz signals were compared by normalizing each spintronic emitter to the reference signal from an InGaAs film.

Temporal form $M(t)$ of ultrafast demagnetization for all the measured pumping energy densities was obtained as a result of approximation of experimental time dependences with expression (1). The maximum demagnetization magnitude was then determined (Fig. 3, *b*, right scale) based on $M(t)$. The value of time constant τ_1 derived from the time dependences of ultrafast demagnetization for Co/WSe_2 falls within the range of $10-40$ fs. Significantly longer demagnetization times were found in the studies of magnetization dynamics of Co films without a semiconductor or a non-magnetic metal [21]. In addition, the demagnetization time for a ferromagnetic/TMD bilayer in [22] is comparable to the one determined in the present study. The demagnetization time reduction is likely a confirmation of the effect of strong spin-orbit coupling emerging at the ferromagnetic/TMD interface [22]. The obtained result demonstrates that ultrafast demagnetization is the dominant mechanism of THz radiation. The maximum magnitude of ultrafast demagnetization is 1.5%.

Thus, a technologically simple method for fabrication of a spintronic emitter based on a ferromagnetic/semiconductor heterostructure was proposed. It was found that the polarization plane of a THz wave may be switched between 0 and 180° by a magnetic field. The proposed emitter demonstrated efficient polarization switching in a coercive field no stronger than 0.1 kOe. The generation of THz radiation in a spintronic emitter based on Co/WSe_2 was characterized as the emission of a time-dependent magnetic dipole. The characteristic times of ultrafast demagnetization confirm that the WSe_2 monolayer affects the THz radiation parameters.

Funding

This study was supported by grant No. 21-79-10353 from the Russian Science Foundation (https://rscf.ru/project/21-79-10353/).

Conflict of interest

The authors declare that they have no conflict of interest.

References

[1] S. Zhong, Front. Mech. Eng., **14**, 273 (2019). DOI: 10.1007/S11465-018-0495-9
[2] M. Seo, H.R. Park, Adv. Opt. Mater., **8**, 1900662 (2020). DOI: 10.1002/ADOM.201900662
[3] J.F. O'Hara, S. Ekin, W. Choi, I. Song, Technologies, **7**, 43 (2019). DOI: 10.3390/TECHNOLOGIES7020043
[4] B.M. Daneshmand, Russ. Technol. J., **9** (5), 14 (2021). DOI: 10.32362/2500-316X-2021-9-5-14-25
[5] L. Yu, L. Hao, T. Meiqiong, H. Jiaoqi, L. Wei, D. Jinying, C. Xueping, F. Weiling, Z. Yang, RSC Adv., **9**, 9354 (2019). DOI: 10.1039/C8RA10605C
[6] A.R. Safin, E.E. Kozlova, D.V. Kalyabin, S.A. Nikitov, Tech. Phys. Lett., **47**, 814 (2021). DOI: 10.1134/S1063785021080241.
[7] C. Bull, S.M. Hewett, R. Ji, C.H. Lin, T. Thomson, D.M. Graham, P.W. Nutter, APL Mater., **9**, 090701 (2021). DOI: 10.1063/5.0057511
[8] T. Kampfrath, M. Battiato, P. Maldonado, G. Eilers, J. Nötzold, S. Mährlein, V. Zbarsky, F. Freimuth, Y. Mokrousov, S. Blügel, M. Wolf, I. Radu, P.M. Oppeneer, M. Münzenberg, Nature Nanotechnol., **8**, 256 (2013). DOI: 10.1038/NNANO.2013.43
[9] E. Vetter, M. Biliroglu, D. Seyitliyev, P. Reddy, R. Kirste, Z. Sitar, R. Collazo, K. Gundogdu, D. Sun, Appl. Phys. Lett., **117**, 093502 (2020). DOI: 10.1063/5.0011009
[10] L. Cheng, X. Wang, W. Yang, J. Chai, M. Yang, M. Chen, Y. Wu, X. Chen, D. Chi, K.E.J. Goh, J.-X. Zhu, H. Sun, S. Wang, J.C.W. Song, M. Battiato, H. Yang, E.E.M. Chia, Nature Phys., **15**, 347 (2019). DOI: 10.1038/s41567-018-0406-3
[11] M. Chen, Y. Wu, Y. Liu, K. Lee, X. Qiu, P. He, J. Yu, H. Yang, Adv. Opt. Mater., **7**, 201801608 (2019). DOI: 10.1002/ADOM.201801608
[12] D.W. Latzke, W. Zhang, A. Suslu, T.R. Chang, H. Lin, H.T. Jeng, S. Tongay, J. Wu, A. Bansil, A. Lanzara, Phys. Rev. B, **91**, 235202 (2015). DOI: 10.1103/PHYSREVB.91.235202
[13] D. Khusyainov, A. Guskov, S. Ovcharenko, N. Tiercelin, V. Preobrazhensky, A. Buryakov, A. Sigov, E. Mishina, Materials, **14**, 6479 (2021). DOI: 10.3390/MA14216479
[14] D. Khusyainov, S. Ovcharenko, A. Buryakov, A. Klimov, P. Pernod, V. Nozdrin, E. Mishina, A. Sigov, V. Preobrazhensky, N. Tiercelin, Phys. Rev. Appl., **17**, 044025 (2022). DOI: 10.1103/PhysRevApplied.17.044025
[15] D. Khusyainov, S. Ovcharenko, M. Gaponov, A. Buryakov, A. Klimov, N. Tiercelin, P. Pernod, V. Nozdrin, E. Mishina, A. Sigov, V. Preobrazhensky, Sci. Rep., **11**, 697 (2021). DOI: 10.1038/S41598-020-80781-5
[16] P. Agarwal, Y. Yang, J. Lourembam, R. Medwal, M. Battiato, R. Singh, Appl. Phys. Lett., **120**, 161104 (2022). DOI: 10.1063/5.0079989
[17] F.A. Zainullin, D.I. Khusyainov, M.V. Kozintseva, A.M. Buryakov, Russ. Technol. J., **10** (3), 74 (2022). DOI: 10.32362/2500-316X-2022-10-3-74-84
[18] N. Kumar, R.W.A. Hendrikx, A.J.L. Adam, P.C.M. Planken, Opt. Express, **23**, 14252 (2015). DOI: 10.1364/OE.23.014252

[19] E. Beaurepaire, G.M. Turner, S.M. Harrel, M.C. Beard, J.-Y. Bigot, C.A. Schmuttenmaer, Appl. Phys. Lett., **84**, 3465 (2004). DOI: 10.1063/1.1737467
[20] L. Cheng, Z. Li, D. Zhao, E.E.M. Chia, APL Mater., **9**, 070902 (2021). DOI: 10.1063/5.0051217
[21] J.Y. Bigot, M. Vomir, L.H.F. Andrade, E. Beaurepaire, Chem. Phys., **318**, 137 (2005). DOI: 10.1016/J.CHEMPHYS.2005.06.016
[22] G. Wu, Y. Ren, X. He, Y. Zhang, H. Xue, Z. Ji, Q.Y. Jin, Z. Zhang, Phys. Rev. Appl., **13**, 024027 (2020). DOI: 10.1103/PHYSREVAPPLIED.13.024027/FIGURES/7/MEDIUM